Do NBTI-Induced Interface States Show Fast Recovery? A Study Using a Corrected On-The-Fly Charge-Pumping Measurement Technique

Ph. Hehenberger*, Th. Aichinger†, T. Grasser•, W. Gös•, O. Triebl•, B. Kaczer‡, and M. Nelhiebel°

* Institute for Microelectronics, TU Wien, A-1040 Wien, Austria † KAI, A-9500 Villach, Austria

• Christian Doppler Laboratory for TCAD at the Institute for Microelectronics, TU Wien, A-1040 Wien, Austria

‡ IMEC, Kapeldreef 75, B-3001 Leuven, Belgium ° Infineon Technologies, A-9500 Villach, Austria

Abstract— **Data obtained by the recently developed on-the-fly charge-pumping technique has suggested a fast initial degradation and recovery of interface states during negative and/or bias temperature stress, contrary to previously published results. By revising the analysis of the measurement setup, fast interface state creation and recovery are revealed as artifact due to a different amount of oxide traps seen during the stress and relaxation phases. From this analysis we conclude that data gathered during stress and recovery phases must not be directly compared. By properly taking the contribution of (slow) oxide charges into account, which leads to a spurious increase of the charge-pumping current during the stress phase, we demonstrate that no fast initial degradation and no fast recovery of interface states occurs. Nevertheless, the charge-pumping signal is sensitive to the continuous switching of the gate voltage into accumulation, which also accelerates interface state recovery, albeit at a slower rate. We finally conclude that both the fast initial degradation and the fast initial recovery seem to be due to oxide charges. Therefore these oxide charges need to be considered. By performing simulations with our device simulator Minimos-NT using a modified Shockley-Read-Hall model it was possible to reproduce the effect of these oxide charges. For this purpose a temperature and field activated tunneling process is assumed and results in proper agreement of measurement and simulation. A correction scheme for the on-the-fly charge-pumping measurement technique is then presented.**

I. Introduction

The last years have seen a lively debate on whether interface states and/or oxide charges are responsible for the degradation observed during negative and/or positive bias temperature stress (NBTI, PBTI). Experimental differentiation between oxide and interface states is extremely challenging due to the rapid recovery of the degradation setting in as soon as the stress is removed. In particular, it has been observed that when after NBTI stress the device is positively biased, a considerable part of the recoverable component is lost [1–4]. Until recently, this has been explained by the detrapping of holes [2, 3], while interface states have been assumed to only change their occupancy but do not recover.

A quite striking result obtained with on-the-fly charge-pumping (OFIT) measurements is that in contradiction to conventional charge-pumping (CCP) measurements, OFIT data suggest a considerable amount of fast initial recovery of interface states. We note that this fast initial recovery is not explicitly measured, but is only inferred from the differences between the last stress and the first recovery measurement. Nevertheless, this misconception is a fundamental dilemma and a major issue for our understanding of BTI. Clarification of this matter is the prime requisite for the development of a reliable model. In the following we try to resolve the issue whether interface states do recover quickly ($< 1\,\mathrm{s}$) or not.

II. Experimental Methodology

Unfortunately, experimental validation of the fast recovery behavior is challenging because the technique that is conventionally used to directly measure interface states is the charge-pumping (CCP) technique, which inherently relies on a bias switch into accumulation. Consequently, it is unclear whether the often observed weak recovery in CP data is a consequence of the fact that interface states do not recover or whether this is an artifact of the measurement technique brought about by the strong bias switch.

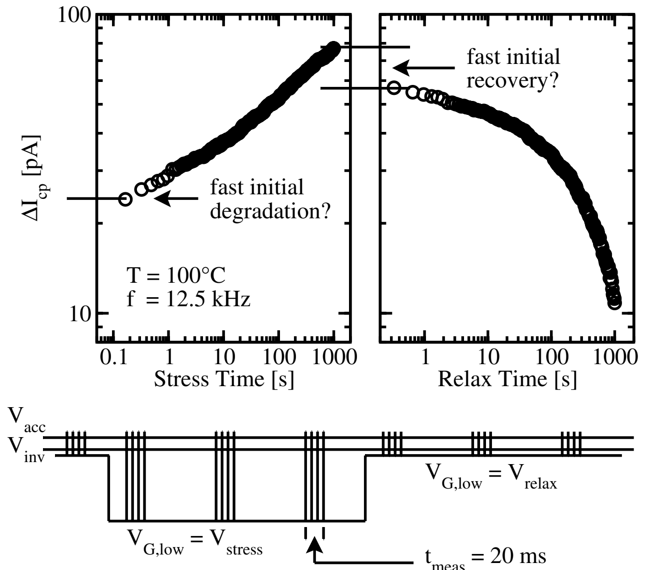

Fig. 1: Typical NBTI stress and relaxation measurement of the charge-pumping current I_{cp} using the OFIT technique with a duty cycle of $50\,\%$. Each symbol in the upper graph is made up of same hundred averaged pulses as schematically displayed in the lower graph for some points. After the reference measurement $V_{\mathrm{G,low}}$ is set to V_{stress}, in order to continuously stress the device. To perform CP, V_{G} is pulsed to V_{acc} periodically. In this way the CP measurement and the application of stress are carried out consecutively. During relaxation $V_{\mathrm{G,low}} = V_{\mathrm{relax}}$. Constant slopes of the stress and relaxation pulses are ensured [5].

The lately developed OFIT technique [6–8] has refueled the debate. As illustrated in Fig. 1, the basic difference between OFIT and CCP [9–12] is that the low-level $V_{\mathrm{G,low}}$ of the CP pulse is simultaneously used as a stress condition (for NBTI), while the actual CP measurement is performed by quickly switching back and forth between accumulation V_{acc} and stress V_{stress}. Consequently, an issue we will get back to later, the low-levels are different during stress and recovery/reference measurements.

III. OFIT versus CCP

As in conventional CP measurements, care has to be taken that parasitic tunneling currents and geometry effects do not pollute the measured charge-pumping current I_{cp}. The first problem is even

978-1-4244-2889-2/09/$25.00 ©2009 IEEE

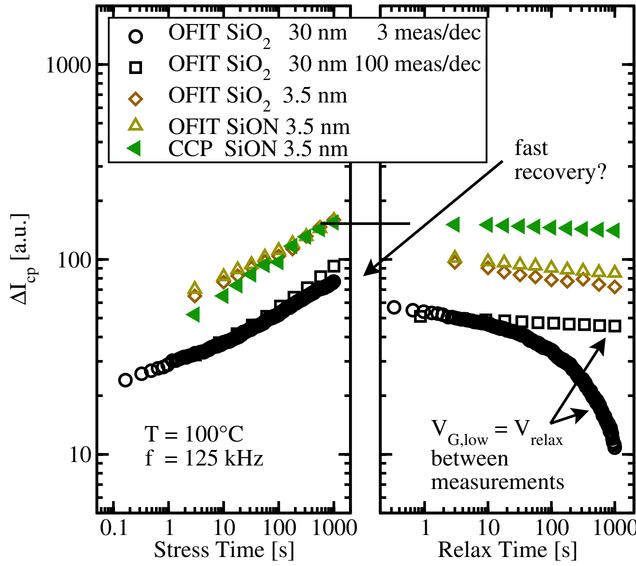

Fig. 2: Comparison of OFIT and CCP results. For OFIT the offset between end of stress and beginning of relaxation is comparable for different technologies and geometries (not shown). Previously this was explained by fast recovery. This fast recovery is absent in CCP (indicated for SiON). Furthermore, continuous gate pulsing affects both stress and relaxation, causing a faster recovery of interface states with increasing number of measurements (black circles vs. black squares - both of 30 nm OFIT).

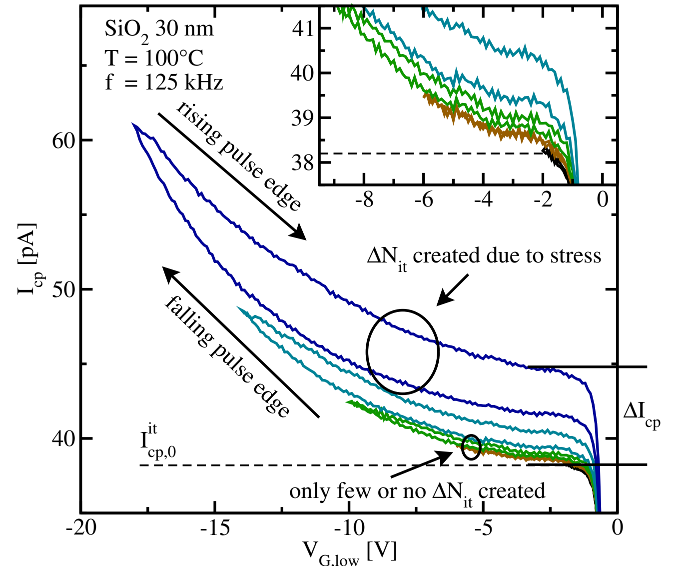

Fig. 3: Charge-pumping current I_{cp} for different pulse amplitudes as observable in constant base-level CP measurements with $V_{\mathrm{Base}} = 2\,\mathrm{V}$ and a gradually increasing pulse amplitude ΔV_{G} from $V_{\mathrm{G,low}} = -1\,\mathrm{V}$ down to $V_{\mathrm{G,low}} = -17\,\mathrm{V}$. The I_{cp} shows a significant hysteresis. If the I_{cp} is evaluated at the falling pulse edge, the lower branch of the curve is traversed. Evolution of the rising pulse edges gives the upper branch. However, the contribution of slow oxide states and an additional hysteresis (marked with ΔI_{cp}) are clearly visible for increasing pulse amplitudes. This implies that depending on the pulse amplitude, I_{cp} will contain contributions in addition to the interface states. Provided only interface states are available, I_{cp} should be independent of the pulse amplitude (dashed line of $I^{\mathrm{it}}_{\mathrm{cp},0}$).

more severe in the OFIT technique since there the low level gate voltage equals the stress voltage, resulting in excessive tunneling in thin oxides. In order to avoid these problems we also use large-area devices with thick oxides (30 nm). As shown in Fig. 2, the measured I_{cp} during stress and recovery are qualitatively identical for three completely different technologies (30 nm thick $\mathrm{SiO_2}$, 3.5 nm thin $\mathrm{SiO_2}$, and SiON).

Quite remarkably, continuous application of OFIT pulses (as well as CP measurements) has a dramatic impact on both the stress and the recovery characteristics. In particular, with 3 measurements per decade, I_{cp} is quasi constant during recovery, while up to 100 measurements per decade result in approximately 80% recovery of I_{cp}. Another fact worth mentioning is that the first OFIT measurement point during stress is already responsible for at least 30% of the total degradation. Likewise, the first measurement taken during recovery at 300 ms already shows 30% recovery while the rest of the recovery depends basically on the number of measurements per decade.

IV. Analysis of the OFIT Technique

In order to deepen our understanding of the method we performed constant base-level CP measurements ($V_{\mathrm{Base}} = 2\,\mathrm{V}$) using a gradually increasing pulse amplitude ΔV_{G}. Until reaching the desired stress-level starting from $-1\,\mathrm{V}$ down to $-18\,\mathrm{V}$ the pulse slopes have to be kept constant to obtain comparable results. Constant pulse slopes ensure that the upper and lower energy boundaries of the active energy interval remain unchanged, although ΔV_{G} increases [5]. Given the requirements of a constant slope and a constant duty cycle, increasing the pulse amplitude ΔV_{G} leads to larger pulses. This means that the rise and fall times have to be adapted at every voltage step. Since it is inevitable to change both the pulse width and also the rise and fall times one has to ask for the potential pitfalls: Are OFIT-data obtained during stress and relaxation comparable? If that is not the case, is there some possibility to correct this nonconformity? These questions will be examined in the following.

Starting with Fig. 3 the two large arrows pointing up and down again reveal some important aspects of the temporal evolution of the pulses during a CP measurement. The charge-pumping current I_{cp} at stress conditions ($V_{\mathrm{G,low}} < -3\,\mathrm{V}$) differs a lot when compared to relaxation ($V_{\mathrm{G,low}} = -1\,\mathrm{V}$). The further the NBTI stress increases the higher the I_{cp}-signal becomes. This can be partly attributed to the desired effect of using the measurement setup to also stress the device. However, this cannot fully account for the observed behavior.

A. Dependence on Gate Voltage Low-Level

Under the assumption that only interface states N_{it} contribute to I_{cp}, I_{cp} should actually become independent of $V_{\mathrm{G,low}}$ as soon as the strong inversion regime is reached. This $I^{\mathrm{it}}_{\mathrm{cp},0}$ is marked by the dashed line in Fig. 3. However, as demonstrated previously [13, 14], I_{cp} continues to increase, albeit at a much slower rate. This increase with ΔV_{G} is routinely attributed to slower oxide traps ΔN_{ot} and $I_{\mathrm{cp}} = I^{\mathrm{it}}_{\mathrm{cp}} + I^{\mathrm{ot}}_{\mathrm{cp}}$ [11, 15]. So, regardless of the amount of degradation, I_{cp} varies as function of $V_{\mathrm{G,low}}$. This fact has to be taken into account for a meaningful comparison of stress and relaxation CP data.

B. Hysteresis due to Stress

When $V_{\mathrm{G,low}}$ is lowered towards the stress voltage, as required in the OFIT technique, I_{cp} extracted from the rising and falling pulse edges start to deviate, introducing a hysteresis. The characteristic hysteresis curve is only visible for larger pulse amplitudes, indicating

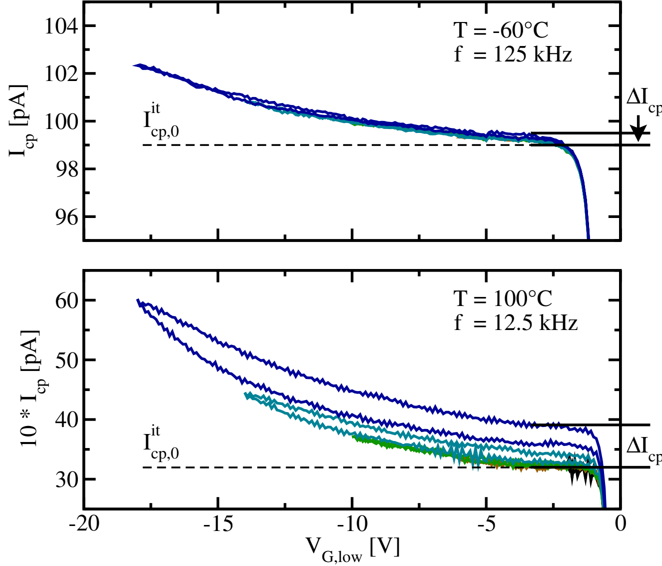

Fig. 4: Top: At a low temperature the hysteresis is negligible (less than 1%) and the contribution of slow oxide traps is reduced. **Bottom**: At a low frequency and a high temperature the contribution of oxide traps increases due to the increased rise and fall times. A comparable if not equal part of interface states constituting ΔI_{cp} can be identified for different frequencies but equal temperature. Following these results at least part of the defects must vary with temperature or frequency. For better comparability, the data at 12.5 kHz are scaled to the reference frequency ($f_{\mathrm{ref}} = 125\,\mathrm{kHz}$).

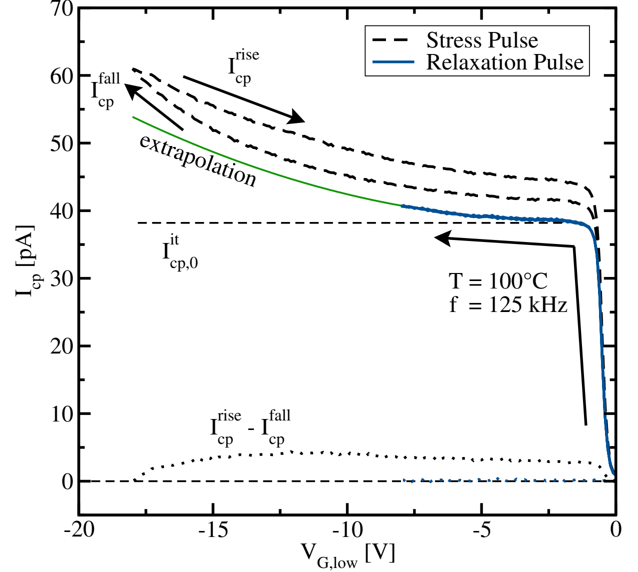

Fig. 5: Charge-pumping current I_{cp} for the stress pulse ($V_{\mathrm{stress}} = -17\,\mathrm{V}$) and the relaxation pulse ($V_{\mathrm{relax}} = -8\,\mathrm{V}$), shown in Fig. 3. To unravel the contribution of oxide charges and additional interface states we look at the difference $I^{\mathrm{rise}}_{\mathrm{cp}} - I^{\mathrm{fall}}_{\mathrm{cp}}$. In the range $-8\,\mathrm{V} < V_{\mathrm{G,low}} < 0\,\mathrm{V}$, this difference is constant, implying no additional creation of interface states. From this 'safe window' we extrapolate to the minimum low-level to estimate the contribution due to oxide charges. Note that the first branches $I^{\mathrm{fall}}_{\mathrm{cp}}$ of the stress and relaxation pulse differ from each other due to pre-stress pulses between $V_{\mathrm{G,low}} = -8\,\mathrm{V}$ and $V_{\mathrm{G,low}} = -17\,\mathrm{V}$. In fact, when using fresh devices for each measurement all $I^{\mathrm{fall}}_{\mathrm{cp}}$ would coincide.

degradation (marked with ΔN_{it} and ΔI_{cp}) due to stress. While the impact of the oxide traps visible during medium $V_{\mathrm{G,low}}$ appears to be fully recoverable, the component causing the hysteresis is not. This can be seen in Fig. 3 where I_{cp} increases during subsequent measurements performed on the same device. We attribute this hysteresis to the creation of additional interface states due to NBTI stress at $V_{\mathrm{G,low}} = V_{\mathrm{stress}}$. Starting at $-2\,\mathrm{V}$ there is nearly no stress. The deeper the device is stressed into inversion the larger the hysteresis becomes, resulting in an increased offset for the next pulse. The total hysteresis at a certain stress level hence not only consists of the hysteresis of the current measurement but is a combination of the previous ones.

C. Hysteresis-Free Area

As displayed in the inset in Fig. 3 the very first pulses are almost free of stress (no hysteresis, $\Delta I_{\mathrm{cp}} = 0$) and hence the deviation of I_{cp} from $I^{\mathrm{it}}_{\mathrm{cp},0}$ is entirely due to oxide traps. Only a negligible amount of interface states ΔN_{it} are created by the measurement process. The hysteresis-free area will be discussed in more detail in the next section.

D. Frequency Scalability

When the experiment is repeated at a lower frequency (see bottom of Fig. 4), one finds that the interface state contribution can be scaled to the reference frequency ($f_{\mathrm{ref}} = 125\,\mathrm{kHz}$) [13]. This is compatible with the fact that the stress duration is practically independent of frequency. On the other hand, the recoverable oxide trap contribution to I_{cp} depends on frequency, consistent with the idea that the lower the frequency (corresponding to more time per pulse) the more oxide traps can contribute to I_{cp}.

E. Lower Temperature

Finally, at a low temperature (displayed at the top of Fig. 4) practically no hysteresis is introduced (no NBTI stress) and also the oxide trap contribution is reduced, consistent with the idea that these traps are due to a thermally activated tunneling mechanism [16] rather than elastic (and thus temperature-independent) hole tunneling [1].

V. Extrapolation of Oxide Trap Contribution

As demonstrated above, during an OFIT measurement we have to expect a distortion of I_{cp} due to oxide charges and due to the creation of defects during the low-level. In order to analyze this distortion we proceed as follows:

We determine $\hat{V}_{\mathrm{G,low}}$ to be the lowest value of $V_{\mathrm{G,low}}$ at which no hysteresis is observed. We then use the data set $V_{\mathrm{G,low}} > \hat{V}_{\mathrm{G,low}}$ to extrapolate the impact of oxide charges ΔN_{ot} down to the stress-level. It is not possible to obtain this information from the stress pulse because of the contribution of both parts: ΔN_{it} and ΔN_{ot}. Quite remarkably, the data can be fit by a quadratic polynomial, consistent with our NBTI experiments where we also observe a quadratic (E^2_{ox}) dependence of the hole-trapping component [16–18]. The hole-trapping theory developed in [16] was applied to our data and excellent agreement was obtained. The difference between the actual signal ($I^{\mathrm{it}}_{\mathrm{cp}} + I^{\mathrm{ot}}_{\mathrm{cp}}$) and the extrapolated curve in Fig. 5 finally gives ΔN_{it}.

In Fig. 5 and Fig. 6 the extraction algorithm for ΔN_{ot} and ΔN_{it} is demonstrated. Stress and relaxation pulse responses both consist of two branches, one going down (fall) and one going up (rise) as marked by arrows. In the falling branch, $V_{\mathrm{G,low}}$ varies from 0 V to

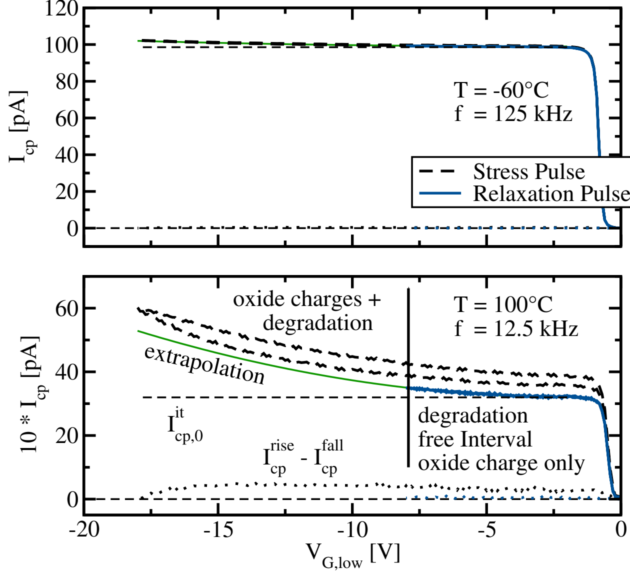

Fig. 6: Top: Lower temperatures simplify the extrapolation due to the absence of degradation. Here the full range of pulse amplitudes can be used to verify the extrapolation down to deep inversion. Very good conformity is obtained, again indicating the absence of additional interface states in deep inversion at low temperatures. **Bottom**: Noise complicates this procedure at low frequencies. Data are scaled to $f_{\text{ref}} = 125\,\text{kHz}$.

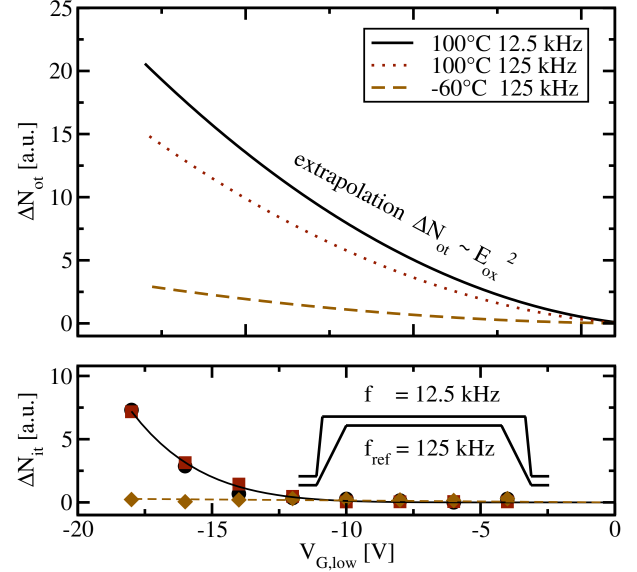

Fig. 7: The extracted oxide states (**Top**) and additional interface states (**Bottom**). The change of oxide trap density ΔN_{ot} follows E_{ox}^2 and furthermore depends on the frequency as well as on the temperature. The hysteresis displayed in the previous figures are due to additionally created traps, ΔN_{it}, which are independent of the frequency but strongly dependent on the temperature.

$-17\,\text{V}$. In the rising branch, $V_{\text{G,low}}$ varies from $-17\,\text{V}$ to $0\,\text{V}$. Only pulses with constant $I_{\text{cp}}^{\text{rise}} - I_{\text{cp}}^{\text{fall}}$ (or even without a hysteresis, i.e. $I_{\text{cp}}^{\text{rise}} - I_{\text{cp}}^{\text{fall}} = 0$) are suitable to create an extrapolation guess for higher $V_{\text{G,low}}$. This 'safe window' ranges from $0\,\text{V}$ to $-8\,\text{V}$ where both branches are indistinguishable.

The extracted components for different temperatures and frequencies are given in Fig. 7. The additionally created oxide traps ΔN_{ot} depend on frequency as well as on temperature and clearly show $V_{\text{G,low}}^2 \sim E_{\text{ox}}^2$ behavior. The hysteresis due to additionally created traps ΔN_{it} is independent of frequency but strongly dependent on temperature.

VI. Simulation of the Charge-Pumping Current

To approximately account for the temperature and field activated tunneling process, we use a modified Shockley-Read-Hall (SRH) model with our device simulator Minimos-NT [19]. The SRH-capture-rates are multiplied by

$$\exp\left(\frac{E_{\text{ox}}^2}{E_{\text{ox,ref}}^2}\right)\exp\left(-\frac{\Delta E_{\text{B}}}{k_{\text{B}}T}\right)$$

where E_{ox} is the electric field in the oxide, $E_{\text{ox,ref}}$ is a reference value, ΔE_{B} the multiphonon emission barrier and T the temperature. ΔE_{B} can be characterized by a Gaussian distribution with the mean energy ΔE_{B}. When setting the parameters some points need to be considered in order to end up with a physically appropriate model:

1) The first exponential factor models the bias dependence. It is very sensitive to changes of $E_{\text{ox,ref}}$ due to the squared exponent, leading to a very small range of valid $E_{\text{ox,ref}}$ values.
2) When setting the barrier ΔE_{B} too low, the oxide traps contribute to the interface trap signal as the second factor approaches unity. Setting ΔE_{B} too high leads to very low rates, effectively eliminating the contribution of oxide traps.
3) Lastly, the distribution of ΔE_{B} determines the dependence of I_{cp} on $V_{\text{G,low}}$. Increasing the mean of the distribution at ΔE_{B} increases the mean capture/emission-time constants. Since with constant-slope pulses higher pulse amplitudes ΔV_{G} require longer pulse durations, increasing the mean ΔE_{B} shifts the point from which a significant contribution of oxide traps ΔN_{ot} can be observed to higher pulse amplitudes. On the other hand, broadening the distribution of ΔE_{B} (increasing the variance) also broadens the distribution of time constants, observable as broadening the range of $V_{\text{G,low}}$ where I_{cp} increases. A quadratic behavior as observed in the experiments, Fig. 8, can be well reproduced with a broad Gaussian distribution ($\Delta E_{\text{B,mean}} = 1\,\text{eV}, \Delta E_{\text{B},\sigma} = 0.5\,\text{eV}$).

Simulation results are depicted in Fig. 8. As the simulation treats the CP measurement process as stress-free, no additional interface traps due to stress are created and only the oxide-charge part is visible. With the thermally activated barrier the increasing ΔI_{cp} can be described.

VII. Results

Based on the previous results we are now able to better understand the charge-pumping current I_{cp} measured during the OFIT sequence. The presence of additional charges contributes to the signal when the pulse amplitude ΔV_{G} is increased. A large spread of time constants slower than that of the interface states is necessary to explain the results. By assuming oxide traps with a thermally distributed activated barrier one is able to explain the measurement results with good accuracy. Whereas interface states are independent of the electric field and account for I_{cp} at low ($10\,\text{kHz}$) and high frequencies ($1\,\text{MHz}$) likewise due to their small time constants, the oxide traps

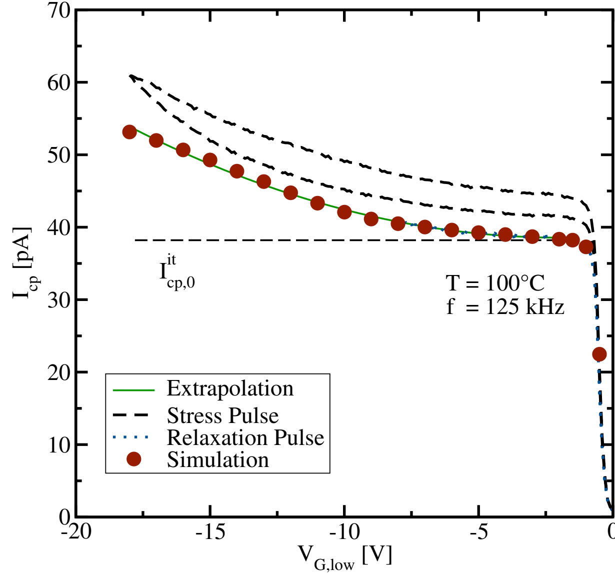

Fig. 8: The contribution due to oxide traps can be well described using the model suggested in [16]. This model assumes that hole-trapping is possible via a multiphonon process implying a thermally activated barrier $\exp(-\Delta E_{\mathrm{B}}/\mathrm{k_B}T)$ and a $\exp(E^2_{\mathrm{ox}}/E^2_{\mathrm{ox,ref}})$ field dependence. We ascertain that the simulation only describes oxide traps and interface traps without applied stress conditions. Additional interface traps due to NBTI stress are missing in the simulation because of a constant number of interface traps for each taken simulation point (solid circles).

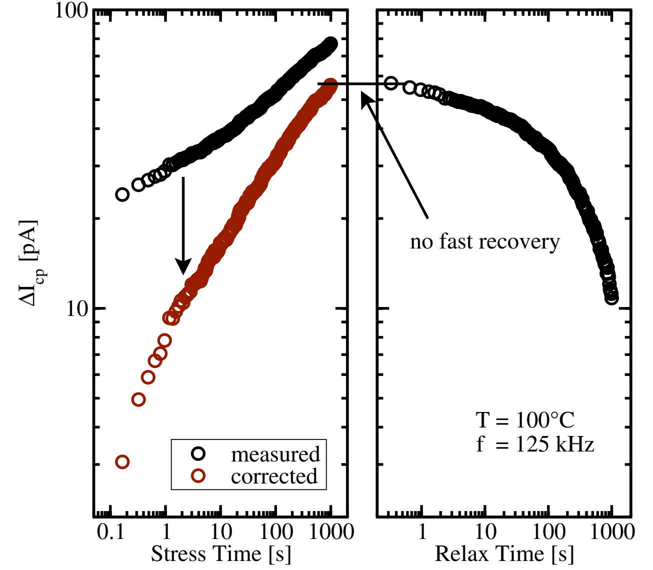

Fig. 9: Oxide traps lead to a spurious increase in the charge-pumping signal during stress. Using the scheme developed for Fig. 1, a corrected I_{cp} is obtained. The smooth transition between the corrected I_{cp} during stress and the I_{cp} during recovery suggests that no fast recovery takes place.

with their assumed barrier are by far slower, only affecting I_{cp} at lower frequencies i.e. 10 kHz.

The particularly troublesome part is the application of the OFIT technique during the stress phase, where both oxide traps ΔN_{ot} and additionally created interface states ΔN_{it} add to I_{cp}. These contributions are absent during the initial reference measurements and during the OFIT recovery measurements both taken at $V_{\mathrm{G,low}} = V_{\mathrm{relax}}$. This has fundamental consequences on OFIT measurements: Initially, a reference I_{cp} is recorded. Following this reference measurement, the gate voltage low-level $V_{\mathrm{G,low}}$ is switched to stress V_{stress}. Due to the much larger ΔV_{G} now a significant contribution of $I^{\mathrm{ox}}_{\mathrm{cp}}$ is obtained.

Furthermore, with the large pulse amplitude, additional interface states are created, which is the intended effect of this OFIT measurement. However, without this the additional increase in I_{cp} due to oxide traps must not be attributed to interface states created by degradation. Consequently, we need to correct for $I^{\mathrm{ot}}_{\mathrm{cp}}$ in the measurement data. Using the mentioned extrapolation method of $\Delta N_{\mathrm{ot}} = AE^2_{\mathrm{ox}}$ we see that the 30% initial increase in I_{cp} is entirely due to oxide traps. The corrected last stress value in Fig. 9 is identical to the first value at the recovery, leading to the conclusion that no fast interface state recovery occurs.

Conclusions

We have discussed the dynamics of interface state creation in constant base-level charge-pumping measurements using a gradually increasing pulse amplitude ΔV_{G} (from inversion into deep inversion). The charge-pumping current is not constant once reaching the inversion regime, but increases due to slow oxide traps. From this analysis we conclude that data gathered during stress and recovery phases must not be directly compared. A correction scheme for the OFIT measurement technique was necessary. By properly taking the contribution of these traps into account, we demonstrate that no fast initial degradation and no fast recovery of interface states occurs. Nevertheless, the CP signal is sensitive to continuous switches of the gate voltage into accumulation which also accelerates interface state recovery, albeit at a slower rate. We finally conclude that both the fast initial degradation and the fast initial recovery are very likely to be due to oxide charges which are created by a thermally activated process.

Acknowledgment

The research leading to these results has received funding from the European Community's Seventh Framework Programme under grant agreement n°216436 (project ATHENIS). We thank Professor Ming-Fu Li, Wenjun Liu and Zhiying Liu for stimulating discussions.

References

[1] M. Denais, V. Huard, C. Parthasarathy, G. Ribes, F. Perrier, N. Revil, and A. Bravaix, "Interface Trap Generation and Hole Trapping under NBTI and PBTI in Advanced CMOS Technology with a 2-nm Gate Oxide," *T-DMR*, vol. 4, pp. 715–722, 2004.

[2] V. Huard, M. Denais, and C. Parthasarathy, "NBTI Degradation: From Physical Mechanisms to Modelling," *Microelectronics Reliability*, vol. 46, no. 1, pp. 1–23, 2006.

[3] V. Huard, C. Parthasarathy, N. Rallet, C. Guerin, M. Mammase, D. Barge, and C. Ouvrard, "New Characterization and Modeling Approach for NBTI Degradation from Transistor to Product Level," in *IEDM*, 2007, pp. 797–800.

[4] T. Grasser, B. Kaczer, and W. Gös, "An Energy-Level Perspective of Bias Temperature Instability," in *IRPS*, 2008, 28-38.

[5] Th. Aichinger and M. Nelhiebel, "Charge Pumping Revisited - The Benefits of an Optimized Constant Base Level Charge Pumping Technique for MOS-FET Analysis," in *IIRW*, 2007.

[6] M.-F. Li, D.M. Huang, C. Shen, T. Yang, W.J. Liu, and Z.Y. Liu, "Understand NBTI Mechanism by Developing Novel Measurement Techniques," *T-DMR*, vol. 8, no. 1, pp. 62–71, March 2008.

[7] W.J. Liu, Z.Y. Liu, D.M. Huang, C.C. Liao, L.F. Zhang, Z.H. Gan, W.S. Wong, C. Shen, and M.-F. Li, "On-The-Fly Interface Trap Measurement and its Impact on the Understanding of NBTI Mechanism for p-MOSFETs with SiON Gate Dielectric," in *IEDM*, 2007.

[8] Z.Y. Liu, D.M. Huang, W.J. Liu, C.C. Liao, L.F. Zhang, , Z.H. Gan, W.S. Wong, and M.-F. Li, "Comprehensive Studies of BTI Degradation in SiON Gate Dielectric CMOS Transistors by New Measurement Techniques," in *IRPS*, 2008.

[9] P. Heremans, J. Witters, G. Groeseneken, and H.E. Maes, "Analysis of the Charge Pumping Technique and its Application for the Evaluation of MOSFET Degradation," *T-ED*, vol. 36, pp. 1318–1335, 1989.

[10] G.V.d. Bosch, G.V. Groeseneken, P. Heremans, and H.E. Maes, "Spectroscopic Charge Pumping: A New Procedure for Measuring Interface Trap Distributions on MOS Transistors," *T-ED*, vol. 38, pp. 1820–1831, 1991.

[11] R.E. Paulsen and M.H. White, "Theory and Application of Charge Pumping for the Characterization of Si-Si02 Interface and Near-Interface Oxide Traps," *T-ED*, vol. 41, pp. 1213–1216, 1994.

[12] D. Bauza, "Rigorous Analysis of Two-Level Charge Pumping: Application to the Extraction of Interface Trap Concentration versus Energy Profiles in Metal-Oxide-Semiconductor Transistors," *J. Appl. Phys.*, vol. 94, pp. 3239–3248, 2003.

[13] G. Groeseneken, H.E. Maes, N. Beltran, and R. F. de Keersmaecker, "A Reliable Approach to Charge-Pumping Measurements in MOS Transistors," *T-ED*, vol. 31, pp. 42–53, 1984.

[14] J.S. Brugler and P. Jespers, "Charge Pumping in MOS Devices," *T-ED*, vol. 16, pp. 297–302, 1969.

[15] Th. Aichinger, M. Nelhiebel, and T. Grasser, "On the Energy Dependence of Oxide Trap Recovery after NBTI Stress," in *IRPS*, 2009.

[16] T. Grasser, B. Kaczer, W. Gös, Th. Aichinger, Ph. Hehenberger, and M. Nelhiebel, "A Two-Stage Model for Negative Bias Temperature Instability," in *IRPS*, 2009.

[17] D.M. Fleetwood, "Fast and Slow Border Traps in MOS Devices," in *RADECS*, 1995.

[18] B. Kaczer, T. Grasser, Ph.J. Roussel, J. Martin-Martinez, R. O'Connor, B.J. O'Sullivan, and G. Groeseneken, "Ubiquitous Relaxation in BTI Stressing New Evaluation and Insights," in *IRPS*, 2008.

[19] IμE, *MINIMOS-NT 2.1 User's Guide*, Institut für Mikroelektronik, Technische Universität Wien, Austria, 2004, http://www.iue.tuwien.ac.at/software/minimos-nt.